Submonolayer structure of an abrupt Al/GaAs{001}-(2×4) interface

J. S. Burnham,* D. E. Sanders,† C. Xu,‡ R. M. Braun, S. H. Goss, K. P. Caffey,§ B. J. Garrison, and N. Winograd
Department of Chemistry, Pennsylvania State University, 152 Davey Laboratory, University Park, Pennsylvania 16802
(Received 22 May 1995; revised manuscript received 29 November 1995)

The structure of As-terminated Al/GaAs{001}-(2×4) has been determined in atomic detail using angle-resolved secondary-ion-mass spectrometry. We find an abrupt interface is formed at room temperature by deposition of 0.3 ML of Al onto GaAs{001}-(2×4) prepared *in situ* by molecular-beam epitaxy. The Al atoms are found to adsorb in the troughs between two As_2 dimers, in ordered sites 0.79±0.10 Å above the surface plane. These dimers maintain their 2.73-Å spacing after Al deposition. The structure is determined from angular distributions of Al^+ and Ga^+ ions desorbed by keV ions and computer simulations of the ion-bombardment event.

I. INTRODUCTION

Elucidation of the structure of the technologically important GaAs{001} surface has been a notoriously difficult endeavor spanning several decades.[1] The situation is complicated by the presence of more than six observed diffraction patterns from GaAs{001}, by the tendency of most metals to disrupt the GaAs surface structure through alloy formation or intermixing, and by the presence of a multicomponent surface with a large unit cell, a problematic circumstance for most surface science techniques. These complexities have continued to frustrate technological initiatives aimed at tailoring Schottky barrier heights of metal-GaAs contacts. Moreover, simple enumeration of the factors that influence the formation of these barriers, such as the reconstruction of the starting surface, has lead to controversy.[2–4]

In spite of these difficulties, significant increases in our knowledge of the structure of clean GaAs surfaces have been achieved recently, particularly with scanning tunneling microscopy (STM). These studies reveal that the classic (2×4) reconstruction involves the formation of As_2 dimers with their bond axis perpendicular to the ⟨110⟩ azimuth (Fig. 1).[5–11] Some of these dimers are found to be missing, most likely because there is an electron deficiency associated with the theoretical GaAs {001}(2×1) reconstruction. As noted in Fig. 1, disagreement has existed over what the most stable (2×4) surface reconstruction is, due to at least two different possibilities observed with STM,[7,12–14] and at least four different theoretical models have been proposed.[5–11] Field-ion-scanning tunneling-microscopy[15] and shadow-cone-enhanced secondary-ion-mass spectrometry (SIMS) (Ref. 16) experiments suggest that the As_2 bond length is reduced to 2.8 and 2.73 Å, respectively, from a bulk value of 4.00 Å. Finally, more recent experimental and theoretical results indicate that the two-dimer model may be more accurate than the three dimer model; however, the structure within the missing As_2 dimer rows has not been confirmed experimentally.[17,18]

Much less information is known about the structure of even the simplest metal overlayers such as Al, the prototypical metal/GaAs system. Although Al adsorption on GaAs has been the focus of many investigations, no approach has yet succeeded in detailing the initial adsorbate positions.[3,4,19–23] Only for Si{001}-(2×1) have these efforts been successful. For instance, Al is found to form linear chains with multiple structural phases.[24] At low coverages, these chains consist of metal dimers bound in the substrate channels with the Al bond oriented parallel to the underlying Si dimers. In this work, we report that at room temperature, Al forms an atomically abrupt overlayer on GaAs{001}-(2×4) at coverages of up to 0.3 ML with Al atoms binding in the channel between the As_2 dimers. In contrast to the Si studies, metal dimerization is not observed. The structure is determined by angle-resolved SIMS measurements of both Ga^+ and Al^+ secondary ions.

II. EXPERIMENT

The experiments were performed in an ultrahigh vacuum (UHV) complex consisting of a Riber 2300 molecular-beam epitaxy (MBE) system and a surface analysis chamber

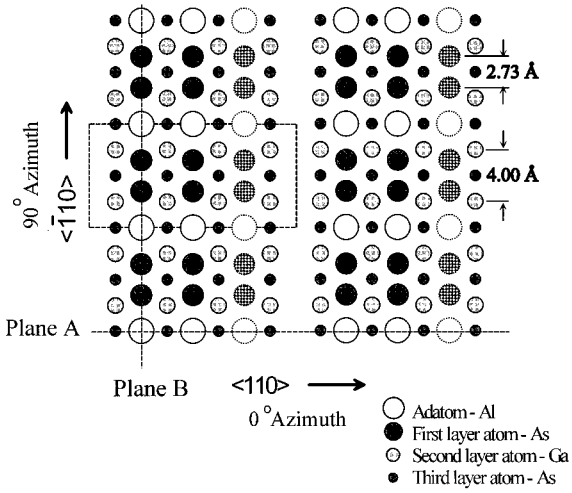

FIG. 1. A schematic of 0.25–0.375 ML of Al adsorbed on GaAs{001}-(2×4), showing the proposed Al adsorption sites. The positions of the substrate atoms are those proposed for the clean GaAs{001}-(2×4). The rows of dotted Al atoms and As atoms are missing in the two-dimer model. The assumed number of missing dimers will affect the number of available adsorption sites for Al, but will not alter the assignments of the desorption mechanisms that give rise to the observed angular anisotropy.

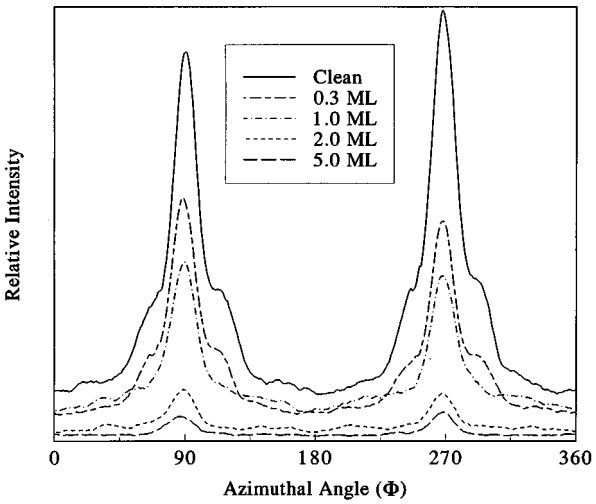

FIG. 2. The experimental angular distribution of 20-eV Ga^+ ions ejected at $\Theta = 45°$ versus Al coverage and azimuthal angle, Φ.

equipped with low-energy electron diffraction (LEED) and angle-resolved SIMS.[16,25] The GaAs{001} wafers were spin etched in a 10:1:1 solution of H_2O:H_2O_2:NH_4OH for 20 s rinsed in distilled water, and bonded to a Mo block with In before insertion into the vacuum system. The native oxides were removed in vacuum by heating to 900 K under As_4 flux. The substrate was then cooled to 860 K and coated with a 5-μm-thick buffer layer. An additional GaAs layer, at least 0.5 μm thick, was grown prior to each Al deposition to ensure a pristine starting surface. Room-temperature As-terminated surfaces with (2×4) periodicity were prepared by cooling from 860 K to 630 K under a reduced As_4 flux. The As_4 flux was discontinued at 630 K and the samples were cooled to 300 K. At this stage of the process, the samples exhibited sharp (2×4) reflection high-energy electron-diffraction (RHEED) patterns in a background pressure of less than 2×10^{-10} torr. Next, a 0.3 ML of Al was deposited at a rate of 0.006 ML/s. One ML of Al is defined relative to the surface site density of the bulk-terminated GaAs{001} crystal face (6.26×10^{14} atoms/cm^2). After Al deposition, the samples retained their (2×4) periodicity with only a slight weakening of the half order streak in the $\langle110\rangle$ direction. The samples were transferred under UHV conditions to the analysis chamber immediately after deposition, whereby LEED analysis also showed that the surface retained its (2×4) periodicity. The angle-resolved SIMS experiments were performed, using 3-keV Ar^+ primary ions at an ion dose of $<1\times10^{13}$ ions/cm^2. Desorbed Al^+ and Ga^+ secondary ions were collected at 20 ± 5 eV. The As^- ion intensity is too small to obtain angle-resolved maps.

III. RESULTS AND DISCUSSION

Angle-resolved SIMS distributions of Ga^+ ions emitted from GaAs{001}-(2×4), as a function of Al converge at a fixed polar angle of $\Theta = 45°$ are shown in Fig. 2. These data are important in ascertaining whether there is an exchange between Al atoms and Ga atoms during the deposition process. Even though exchange of this sort is well documented to occur at high temperatures or on Ga-rich surfaces,[26–28] evidence for exchange at room temperature is sketchy.[21,29–31]

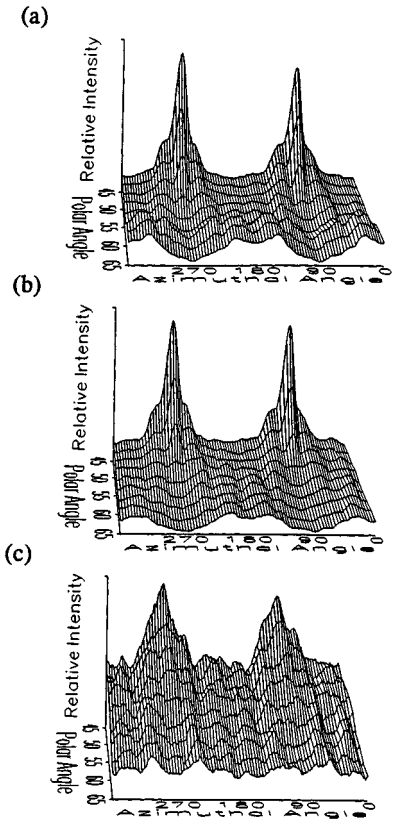

FIG. 3. The experimental angular distributions of 20-eV secondary ions desorbed by normally incident 3-keV Ar^+-ion bombardment. (a) Desorbed intensity of Ga^+ ions from clean GaAs {001}-(2×4). (b) Desorbed intensity of Ga^+ ions from 0.3-ML Al deposited on GaAs{001}-(2×4) at 300 K. (c) Desorbed intensity of Al^+ ions from 0.3 ML Al deposited on GaAs{001}-(2×4) at 300 K.

The data show that the intensity of Ga^+ ions decreases rapidly as a function of Al coverage. After 1 ML of deposition, the intensity along the $\Phi = 90°$ and 270° directions (see Fig. 1 for angle definitions) has been attenuated by more than 60%. This reduction is consistent with molecular-dynamics computer simulations,[32] which suggest there is a 58% decrease in the yield of desorbed particles from 2nd layer to 3rd layer for the 2×4 surface. Hence, the Al overlayer effectively blocks Ga^+ ion emission, a phenomenon that would not occur if there were significant Ga-Al interchange. Note also that the Ga^+ ion signal is almost completely attenuated after two layers of Al deposition. Although these results are qualitative in nature and subject to vagarities in the ionization probability of Ga^+ ions as a function of Al coverage, they are suggestive that Al is forming an abrupt interface at room temperature.

The complete angle-resolved SIMS distributions for GaAs $\{001\}-(2\times4)$ and Al/GaAs{001}-(2×4) are shown in Fig. 3. The origin of the features associated with the Ga^+ ion distribution from the clean surface have been described in detail with the aid of molecular-dynamics (MD) computer simulations of the ion-bombardment event.[25] Briefly, the two largest peaks arise solely from a direct collision between a 3rd layer As atom and a 2nd layer Ga atom causing Ga^+-ion ejection along their common bond direction. The shoulders

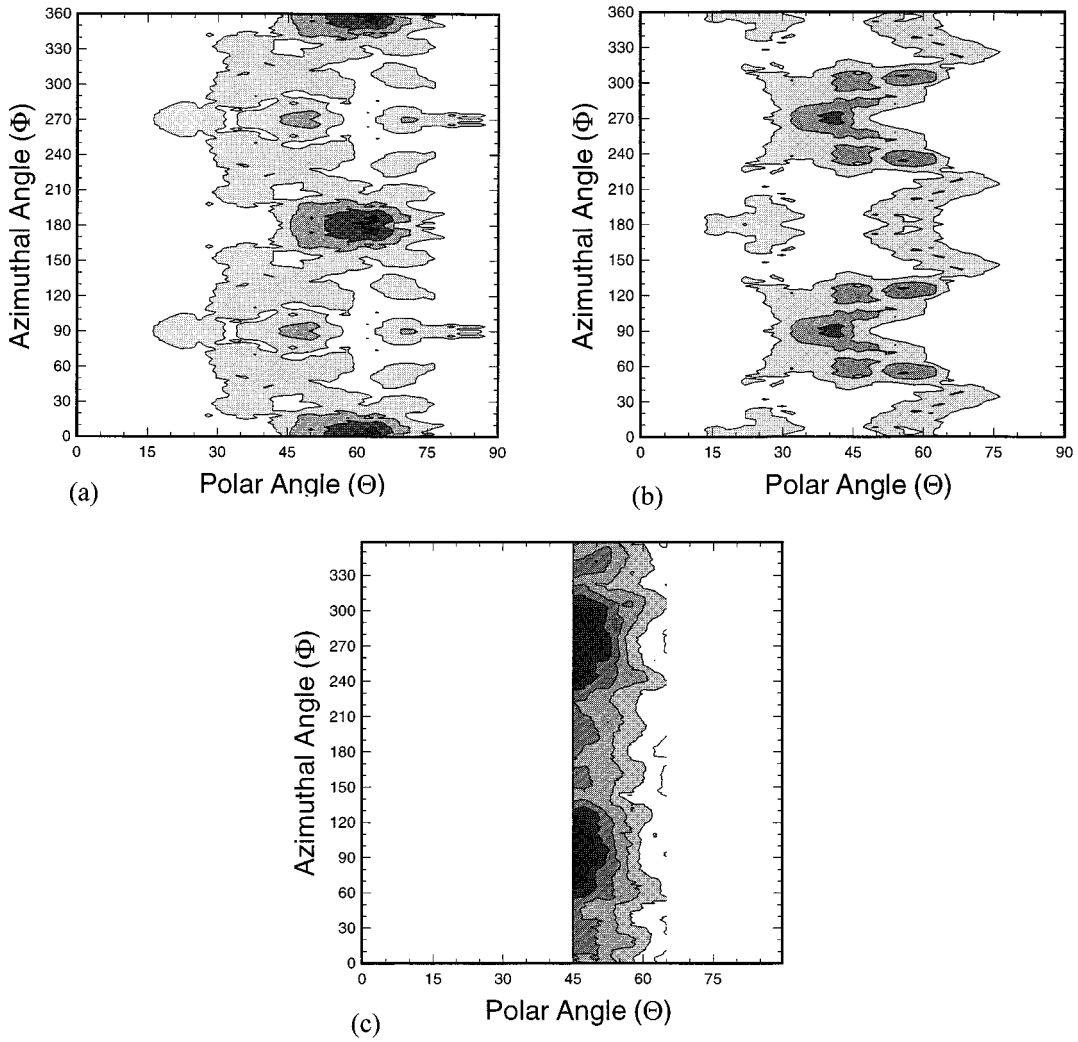

FIG. 4. (a) The calculated angular distribution of 10–30 eV adlayer Al atoms desorbed from the $0.31a_0$ binding height model by 3-keV Ar atom bombardment at normal incidence. (b) The calculated angular distribution of 10–30 eV Al atoms desorbed from the $0.15a_0$ binding height model by 3-keV Ar atom bombardment at normal incidence. (c) The experimental angular distribution of 20-eV secondary Al^+ ions desorbed by normal-incidence, 3-keV Ar^+-ion bombardment of 0.3-ML Al deposited on GaAs{001}-(2×4) at 300 K. The polar angle, Θ, is the angle of detection from the surface normal. For the in-plane azimuthal angle, $\Phi=0°$ corresponds to the $\langle 110\rangle$ crystal direction. The intensities have been multiplied by sin Θ to yield the probability densities. The gray scale uses black as a maximum intensity.

and other features at higher values of the polar angle, Θ, arise from a mix of mechanisms related to the missing row of As_2 and to the formation of the As dimer itself.

Deposition of 0.3 ML of Al onto GaAs{001}-(2×4) reduces the overall intensity of the Ga^+-ion signal by abut a factor of two, as is clear from the data in Fig. 2, but causes almost no change in the shape of the angular distribution, as shown in Fig. 3. This striking observation implies that the most likely sites for Al adatoms are the ones shown in Fig. 1, because these are positions that will not change or redirect ejecting Ga atoms. The assignment is supported by the shape of the Al^+-ion distribution shown in Fig. 3(c), since the two major features along $\Phi=90°$ and 270° would most likely arise from Al^+ ions ejected via a direct transfer of momentum from a first layer As atom to an Al adatom.

Two other features arise in the experimental Al^+-ion distribution shown in Fig. 3(c) that assist in the placement of the Al atoms on the (2×4) surface. The experimental distribution in Fig. 3(c) exhibits peaks at $\Phi=60°$, 120°, 240°, and 300° and at $\Theta=45°$ to 65°. Second, the experimental data in Fig. 3(c) show minor peaks at $\Phi=165°$ and 195° and $\Theta=45°$ to 65°. These two additional features will assist in the assignment of the Al position on the 2×4 surface when utilizing molecular-dynamics computer simulations. Note also that these Al^+-ion features could not occur if Al atoms were significantly displaced from direct alignment with As atoms by Al dimer formation.

It is possible to check qualitatively these ideas using molecular-dynamics computer simulations of the ion-bombardment event. The availability of accurate interaction potentials for use in molecular-dynamics simulations is limited[33] and an appropriate one is not available for Al/GaAs. We have recently shown, however, that it is possible to employ a many-body Si potential developed by Tersoff,[34] to elucidate the mechanistic pathways that give rise to the major features in the angular distribution.[25,32,35] In particular,

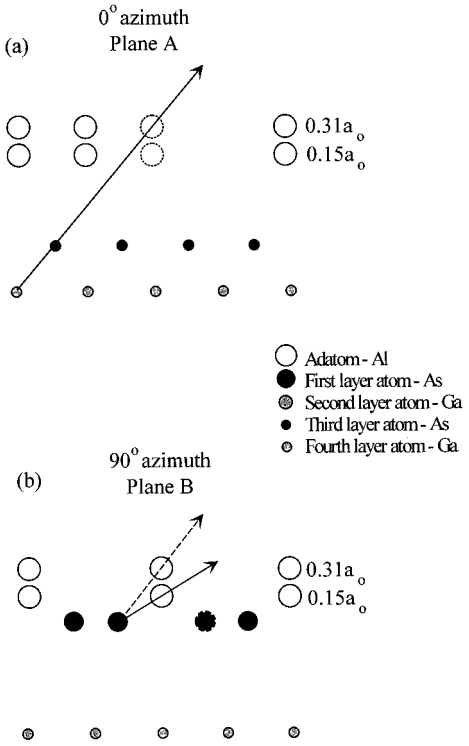

FIG. 5. (a) The side view of plane B in Fig. 1 is shown. The top arrow shows the Δ_3 mechanism for $0.31a_0$. (b) The side view of plane *A* in Fig. 1 is shown. The arrows indicate two types of Δ_1 mechanisms, corresponding to two different Al heights. The top arrow is a small peak, while the bottom is a dominate peak in the simulation.

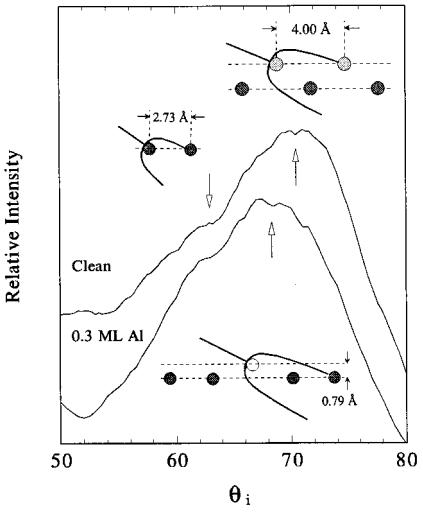

FIG. 6. The relative intensity of Ga^+ ions desorbed from clean and 0.3-ML Al-covered GaAs{001}-(2×4) surfaces, plotted as a function of the angle between the ion beam and the surface normal (Θ_i). The 3-keV Ar^+ ions are incident parallel to the $\langle\bar{1}10\rangle$ crystallographic direction. The insets illustrate the desorption mechanisms associated with each enhanced intensity feature. (○)=Al adatom; (●)=As atom; (⊙)=Ga atom.

a detailed mechanistic study has shown that atoms in diamond lattices primarily eject via two mechanisms.[32] First, the nearest atom in the layer below can eject an atom via a nearest-neighbor collision (Δ_1 mechanism). Second, an atom from three layers below can move unimpeded through crystal and eject a near surface atom (Δ_3 mechanism).

Molecular-dynamics simulations were performed for the proposed structure of the Al on the GaAs surface, using the Si interaction potential. Two heights of the adsorbate atom were used. In the first case, the Al atom was placed $0.31a_0$ above the dimer plane, which is slightly higher than the epitaxial position of an unreconstructed surface ($a_0=5.43$ Å for Si). In the second case, the Al atom was placed only $0.15a_0$ above the dimer plane.

The results of these calculations for the Al angular distributions, along with the appropriate experimental data, are shown in Fig. 4. The data are shown in a contour map format rather than in the three-dimensional format used in Fig. 3, due to the lower density of points available from the calculation. Note that when the Al atom is $0.31a_0$ above the dimer plane, the calculation predicts that there should be pronounced Al intensity along $\Phi=0°$ and 180°. This intensity arises from direct collisions between a third layer As atom and adlayer of Al atom [this is a Δ_3 mechanism, as illustrated in Fig. 5(a)]. When the Al atom is placed $0.15a_0$ above the dimer plane, however, this Δ_3 mechanism is not possible, and the observed intensity along $\Phi=0°$ and 180° drops to nearly zero, as shown in Fig. 4(b) and Fig. 5(a).

An opposite trend is observed for the Δ_1 mechanism, where a surface As atom moving along either the $\Phi=90°$ or the 270° azimuths strikes a surface Al atom, as shown in Fig. 5(b). At the higher Al height, the As atom moves largely under the Al atom. At the lower height, however, there is a direct collision leading to an enhanced Al^+-ion intensity along these directions. For this case, there are a pair of shoulders at $\Theta\leqslant60°$, which are due to blocking by a neighboring As atom [highlighted in Fig. 5(b)].

The experimental data shown in Fig. 4(c) closely matches the situation where the Al atom is placed $0.15a_0$ above the surface plane. Note that there is a maximum in intensity along $\Phi=90°$ and 270° and that the shoulders predicted to occur along these directions are clearly visible. Given the unknown correction factors that might be required in transferring the model calculations from Si to Al/GaAs and from neutral species to ions, it is not appropriate to repeat the calculations at other heights in order to best fit the experimental data. We have checked a number of other candidate structures including two that are representative of structures in which Al adatoms are dimerized. For example, we simulated the adatom dimer bound to the surface a distance $0.15a_0$ and $0.31a_0$ above the As dimer plane. Neither of these dimerized structures yield results that have the direct ejection features caused by the As dimers hitting the Al adlayer t $\Phi=90°$ and 270°. Both of these structures yield results that have the direct ejection feature symmetrically split 20° each side of $\Phi=90°$ and 270°. From the qualitative similarity between Figs. 4(b) and 4(c) of peak heights and peak positions, it appears that we can approximate the relative atomic positions, using these simulations. Hence, the large trough created by the As dimers allow the Al atoms to bond close to the surface in a more planer and nondimerized form.

With knowledge of the rough atomic structure, it is possible to obtain more accurate bond distances using shadow-cone enhanced SIMS. With this approach, the angle of inci-

dence of the ion beam is varied, so that the high flux edge of the shadow cone of a surface atom sweeps across neighboring atoms.[36] When the edge intersects these atoms, an enhancement of the secondary-ion yield is observed. The results obtained from bombarding clean and Al/GaAs{001}-(2×4) at various angles of incidence along the $\langle 110\rangle$ direction are shown in Fig. 6. For the clean surface,[16] the major peak at $\Theta_i = 70.1°$ arises from a Ga-Ga interaction in the second layer and corresponds with the bulk spacing of 4.00 ± 0.10 Å. The shoulder at $\Theta_i = 63.0°$ is associated with the first-layer As-As interaction and corresponds to a spacing of 2.73 ± 0.10 Å, as reported previously.[37] For the Al-covered sample, there is no significant change in the As_2 dimer feature, indicating that the As-As bond distance remains at 2.73 Å. Moreover, there is a peak at 68.3° that arises from an interaction between the shadow cone created by an Al adatom and the As atom on the far side of the dimer. By utilizing the previously described procedure for determination of the shadow-cone shape,[16,37] we calculate the height of Al above the As_2 surface dimer plane to be $(0.79\pm0.1$ Å or $0.14a_0$ for GaAs.

IV. CONCLUSION

In summary, the essential details of the structure of Al/GaAs{001}0(2×4) formed at room temperature have been determined. The results show that Al adatoms incorporate into the GaAs{001}-(2×4) template without significant disruption and the Al adatoms do not dimerize. This model is in direct contrast to the Ga-rich GaAs{001} surface, where the surface Ga atoms are dimerized. The reason for the difference is the high temperatures (>600 K) at which Ga-rich surfaces are prepared. Current experiments suggest that heating the Al/GaAs{001}-(2×4) structure compromises the abrupt nature of the interface and causes As diffusion from the bulk.[38] A further note is that the behavior of Al/Ga interface is quite different than Al/Si{001}-(2×1) prepared at 300 K, where the Al adatoms themselves are found to dimerize. The lattice constants of Si and GaAs are similar, and it is interesting that Al is found to dimerize on Si, but not on GaAs. Apparently, the higher electron density present at the surface on GaAs adequately stabilizes any dangling Al orbitals. Our proposed structure provides an excellent pedestal for the growth of bulk Al ($a_0 = 4.05$ Å) along either $\langle 110\rangle$ or $\langle 001\rangle$, a phenomenon observed recently.[17] Finally, we note that the use of ion-bombardment techniques can provide a direct approach to the solution of rather complex surface structures. In fact, we hope that the results presented here can now be further refined using more sophisticated diffraction techniques (i.e., LEED) or by surface-extended x-ray-absorption fine structure and its related methods.

ACKNOWLEDGMENTS

The authors appreciate many helpful discussions with R. Blumenthal, R. Willis, and K. B. S. Prasad. We thank R. Taylor for her valuable help in performing the MD calculations. The financial support of the National Science Foundation and the Office of Naval Research are gratefully acknowledged. The MD calculations were performed on an IBM RS 6000 computer, purchased via an NSF instrumentation grant and the IBM SUR Program. Additional computer time was provided by The Pennsylvania State University.

*Present address: IBM, Essex Junction, VT.
†Present address: Horizon Systems Inc., Stamford, CT.
‡Present address: ABB, Power T&D Co., Philadelphia, PA.
§Present address: MCNC, Research Triangle Park, NC.

[1] A. Y. Cho, J. Appl. Phys. **47**, 2841 (1976).
[2] C. J. Spindt, M. Yamada, P. L. Meissner, K. E. Miyano, T. Kendelewicz, A. Herrera-Gomez, W. E. Spicer, and A. J. Arko, Phys. Rev. B **45**, 11 108 (1992).
[3] W. I. Wang, J. Vac. Sci. Technol. B **1**, 574 (1983).
[4] M. Missous, E. H. Rhoderick, and K. E. Singer, J. Appl. Phys. **60**, 2439 (1986).
[5] J. Sudijono, M. D. Johnson, C. W. Snyder, M. B. Elowitz, and B. G. Orr, Phys. Rev. Lett. **69**, 2811 (1992).
[6] J. E. Northrup and S. Froyen, Phys. Rev. Lett. **71**, 2276 (1993).
[7] M. D. Pashley and K. W. Haberem, in *Semiconductor Interfaces at the Sub-Nanometer Scale*, Vol. 243 of *NATO Advanced Study Institute, Series E: Applied Sciences*, edited by H. W. M. Salemiak and M. D. Pashley (Kluwer, Dordrecht, 1993), p. 63.
[8] D. K. Biegelson, R. D. Bringons, J. E. Northrup, and L.-E. Swartz, Phys. Rev. B **41**, 5701 (1990).
[9] D. J. Chadi, J. Vac. Sci Technol. A **5**, 834 (1987).
[10] M. D. Pashley, K. W. Haberera, W. Friday, J. M. Woodall, and P. D. Kirchner, Phys. Rev. Lett. **60**, 2176 (1988).
[11] T. Ohno, Phys. Rev. Lett. **70**, 631 (1993).
[12] J. Falta, R. M. Tromp, M. Copel, G. D. Pettit, and P. D. Kirchner, Phys. Rev. Lett. **70**, 3173 (1993).
[13] R. Maboudian, V. Bressler-Hill, and W. H. Weinberg, Phys. Rev. Lett. **70**, 3172 (1993).
[14] L. D. Broekman, R. C. G. Leckey, J. D. Riley, A. Stampfl, B. F. Usher, and B. A. Saxton, Phys. Rev. B **15**, 17 795 (1995).
[15] H. Xu, T. Hashizume, and T. Sakurai, Jpn. J. Appl. Phys. **32**, 1511 (1993).
[16] C. Xu, K. P. Caffey, J. S. Burnham, S. H. Goss, B. J. Garrison, and N. Winograd, Phys. Rev. B **45**, 6776 (1992).
[17] J. E. Northrup and S. Froyen, Phys. Rev. B **50**, 2015 (1994).
[18] T. Hashizume, Q. K. Xue, J. Zhou, A. Ichimiya, and T. Sakurai, Phys. Rev. Lett. **73**, 2208 (1994).
[19] Y. S. Luo, Y.-N. Yang, J. H. Weaver, L. T. Florez, and C. J. Palmstrom, Phys. Rev. B **49**, 1893 (1994).
[20] C. J. Kiely and D. Cherns, Philos. Mag. A **59**, 1 (1989).
[21] G. Landgren, S. P. Svensson, and T. G. Anderson, Surf. Sci **122**, 55 (1982).
[22] P. M. Petroff, L. C. Feldman, A. Yu. Cho, and R. S. Williams, J. Appl. Phys. **52**, 7317 (1981).
[23] J. Mizuki, K. Akimoto, I. Horisawa, K. Hirose, T. Mizutani, and J. Matsui, J. Vac. Sci. Technol. B **6**, 31 (1988).
[24] J. Nogami, A. A. Baski, and C. F. Quate, Phys. Rev. B **44**, 1415 (1991).
[25] R. Blumenthal, K. P. Cafey, E. Furman, B. J. Garrison, and N. Winograd, Phys. Rev. B **44**, 12 830 (1991).
[26] S. A. Chamber, Phys. Rev. B **39**, 12 664 (1989).
[27] X. M. Ding, G. S. Dong, X. K. Lu, H. Y. Xiao, P. Chen, and X. Wang, Appl. Surf. Sci. **41/42**, 123 (1989).
[28] M. Turowski and G. Margaritando, Phys. Rev. B **30**, 3294 (1984).
[29] J. Massies and N. T. Linh, Surf. Sci. **114**, 147 (1982).

[30] G. Landgren and R. Ludeke, Solid State Commun. **37**, 127 (1981).
[31] T. G. Anderson, S. P. Svensson, and G. Landgren, J. Phys. C **15**, 6673 (1982).
[32] D. E. Sanders, K. B. S. Prasad, J. S. Burnham, and B. J. Garrison, Phys. Rev. B **50**, 5358 (1994).
[33] B. J. Garrison and D. Srivastava, Annu. Rev. Phys. Chem. **46**, 373 (1995).
[34] J. Tersoff, Phys. Rev. B **38**, 9902 (1988).
[35] R. Smith, D. E. Harrison, Jr., and B. J. Garrison, Phys. Rev. B **40**, 93 (1989).
[36] N. Winograd, J. Burnham, and C. Xu, Acct. Chem. Res. **27**, 37 (1994).
[37] C. Xu, J. S. Burnham, R. M. Braun, S. H. Goss, and N. Winograd, Phys. Rev. B **52**, 5172 (1995).
[38] S. H. Goss, J. S. Burnham, K. B. S. Prasad, B. J. Garrison, and N. Winograd (unpublished).